

# Spontaneous Ripple Formation in MoS<sub>2</sub> Monolayers: Electronic Structure and Transport Effects

Pere Miró,\* Mahdi Ghorbani-Asl, and Thomas Heine

During the first decades of the 20<sup>th</sup> century, physicists concluded that two-dimensional (2D) materials did not exist since they were thermodynamically unstable and in consequence would not be stable at any finite temperature.<sup>[1,2]</sup> Their arguments were based on the effect of thermal fluctuations on these materials and were strongly supported by experimental evidence.<sup>[3]</sup> In 1962 Hanns-Peter Boehm described single-layer carbon foils and coined the term graphene,<sup>[4]</sup> but Nobel laureates Novoselov and Geim were the main developers behind its routine production and use as a 2D material.<sup>[5,6]</sup> Electron microscopy revealed small ripples in graphene monolayers as a consequence of thermal vibrations.<sup>[7,8]</sup> On one hand, these observations were in perfect agreement with the evidence that a pure 2D lattice could not exist at temperatures above absolute zero. On the other hand, the existence of quasi-2D materials was demonstrated. After this discovery, other 2D materials rapidly emerged such as boron nitride (BN)<sup>[9,10]</sup> and transition metal dichalcogenides (TMDs), including WS<sub>2</sub> and MoS<sub>2</sub>.<sup>[11–13]</sup> Even though graphene has revolutionized the 2D materials field, a deeper understanding of the physics behind other systems is fundamental for their practical application.

One of the most promising 2D materials is MoS<sub>2</sub>, since its structure is composed of sheets stacked on the top of one another. The weak interaction between the layers allows their exfoliation down to monolayers through micromechanical cleavage<sup>[14]</sup> or liquid phase exfoliation.<sup>[11,15]</sup> This material has been used in a wide range of applications such as catalysis,<sup>[16–18]</sup> optoelectronics,<sup>[19,20]</sup> photovoltaics and as a lubricant.<sup>[21]</sup> Recently MoS<sub>2</sub> monolayers were used to realize a field effect transistor with a room-temperature current on/off ratio exceeding  $1 \times 10^8$  and mobility comparable to thin silicon films or graphene nanoribbons.<sup>[22]</sup>

Recently the Kis group reported the microscopic structure of thin layers of MoS<sub>2</sub> using high-resolution transmission electron microscopy (HRTEM) and optical and atomic force microscopy (AFM).<sup>[23]</sup> Analogous to graphene and boron nitride, MoS<sub>2</sub> monolayers were experimentally determined to present ripples. Here, we report the first study on the intrinsic dynamics of MoS<sub>2</sub> monolayers, ripple formation effects on the electronic structure, and the conductance of this material. The full computational details of this work are given in the Supporting Information. In summary, we have used density functional based tight-binding

method (DFTB) in conjunction with Born-Oppenheimer molecular dynamics to explore the ripple formation in MoS<sub>2</sub>.

We have considered five different super cells of increasing size starting from 28.4 Å × 16.2 Å (9 × 6) up to 91.7 Å × 16.2 Å (29 × 6) with a small rigid section required for the conductance calculations. These systems were thermally equilibrated during 10 ps using the NVT ensemble and the dynamics were then studied for an additional 100 ps. On one hand, the small systems (9 × 6 and 14 × 6) did not present a significant change in their structure during the simulations. On the other hand, all of the systems larger than 19 × 6 rapidly showed spontaneous ripple formation (Figure 1). The maximum ( $\lambda_{\max}$ ) and the average ( $\langle\lambda\rangle$ ) ripple height during the DFTB simulations increases monotonically with respect to the system size (Table 1). The maximum rippling is directly influenced by the supercell size since the lattice parameters remain constant during the simulations. In practice the distance between the two rigid regions is the main constraint on the maximum and average rippling during our simulations; however, simulations without restrictions show similar  $\lambda_{\max}$  and  $\langle\lambda\rangle$  values when compared to the ones presented in Table 1.

Brivio et al. determined experimentally that the length ( $L$ ) and  $\langle\lambda\rangle$  of the ripples in MoS<sub>2</sub> monolayers are 60–100 Å and 6–10 Å respectively.<sup>[23]</sup> These results are in perfect agreement with the results of the largest simulated system (29 × 6) which has  $\langle\lambda\rangle = 7.59$  Å and length  $L = 91.7$ . The observed rippling has its origin in the kinetic energy of the system that is directly related to the temperature. We simulated equivalent systems at low temperature and at high temperature. The average ripples increase with the temperature e.g.  $\langle\lambda\rangle$  is 3.49 Å, 3.80 Å and 4.26 Å at 98 K, 298 K and 498 K respectively for the 19 × 6 system. The estimated ripple oscillation frequencies also increase from 110 GHz, 130 GHz and 160 GHz (see Supporting Information for details).

It has been previously demonstrated both experimentally and computationally that monolayers of MoS<sub>2</sub> are semiconductors with a direct bandgap on the order of 1.8 eV.<sup>[20,24]</sup> Our DFTB simulations suggest that at room temperature, the thermal energy rapidly breaks monolayer symmetry inducing a reduction in the bandgap. The most rippled structures during the simulations are an extreme case since the increase of  $\lambda_{\max}$  and  $\langle\lambda\rangle$  leads to an increase in the bandgap reduction (Table 1).

Dr. P. Miró, M. Ghorbani-Asl, T. Heine  
School of Engineering and Science  
Jacobs University Bremen Campus Ring 1  
28759 Bremen, Germany  
E-mail: p.miro@jacobs-university.de



DOI: 10.1002/adma.201301492

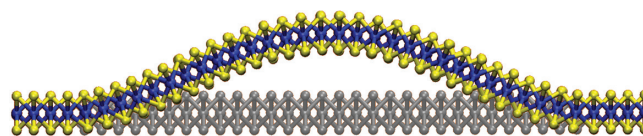


Figure 1. Rippled MoS<sub>2</sub> monolayer during the simulation. In gray the initial flat monolayer. Color code: Molybdenum in blue and sulfur in yellow.

**Table 1.** System length ( $L$ ), maximum ( $\lambda_{\max}$ ) and average heights ( $\langle\lambda\rangle$ ) of the ripples and bandgap of the most rippled monolayer during the simulations. In parentheses the scaled gap.<sup>a)</sup>

Monolayer	$L$ [Å]	$\lambda_{\max}$ [Å]	$\langle\lambda\rangle$ [Å]	Bandgap <sup>b)</sup> [eV]
$9 \times 6$	28.5	0.13	0.01	1.85 (1.43)
$14 \times 6$	44.3	0.21	0.04	1.74 (1.30)
$19 \times 6$	60.1	7.58	3.80	1.45 (1.05)
$24 \times 6$	75.9	11.18	5.96	1.33 (0.95)
$29 \times 6$	91.7	14.47	7.59	1.28 (0.86)
Exp. <sup>[23]</sup>	60–100	-	6–10	$\approx 1.8$ <sup>[20,24]</sup>

<sup>a)</sup>Scaled to reproduce the DFT bandgap for the flat monolayer; <sup>b)</sup>DFTB overestimates the bandgap, e.g., a perfectly flat MoS<sub>2</sub> bandgap is  $\approx 2.1$  eV.

In our simulations, the distance between the rigid sections in the initial flat structures is  $(n-m)$  times the vector  $a$  in the MoS<sub>2</sub> unit cell (where  $m$  is the number of rigid unit cells). The supercell vectors are kept constant during the simulation; however, the rippling increases the distance that must be overcome between the rigid sections. In consequence, the monolayers have to elongate/stretch to ripple and, as our group has recently reported, the stretch or compression of MoS<sub>2</sub> monolayers induces an increase in the bandgap reduction.<sup>[25]</sup> The effect of the rippling on the MoS<sub>2</sub> electronic structure was also studied through the calculation of the total and partial density of states (DOS) (Figure 2). The partial DOS reveals that the major contributions to both valence and conduction bands comes from the molybdenum centers, meanwhile the sulfur only contributes by ca. 10%. We plotted the orbital projected DOS to shed some light onto the orbital compositions of these bands, showing that they contain almost exclusively molybdenum  $4d$  and sulfur  $3p$  orbital contributions (see Supporting Information for details).

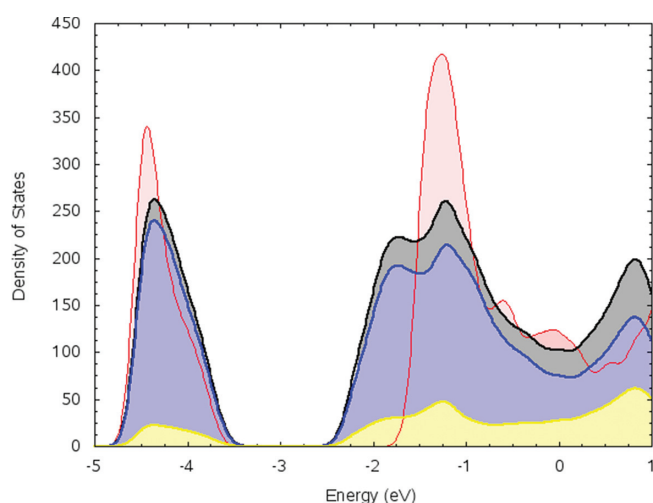


**Figure 2.** Density of states of the  $29 \times 6$  initial (red) and rippled monolayer (black) and partial density of states of molybdenum (blue) and sulfur (yellow) in the rippled monolayer. Bandgap is reduced from 2.1 to 1.28 eV when the monolayer is rippled.

The bandgap reduction due to the bending of the structure is also observed in the total and partial DOS, and we are able to identify its origin. On one hand the Fermi level remains almost unaltered in all of the studied systems independent of system size or bending. On the other hand, the rippling shifts down a considerable portion the conduction band inducing the observed bandgap reduction. The contributions to the new conduction band are equivalent to the ones observed in the partial DOS of the flat monolayers (Figure 2).

The rigid section in the monolayers was divided into two semi-infinite electrodes (Figure 3 top). The electron conductance in the initial monolayer and in the most rippled structure from the simulations was calculated self-consistently using the Green's function formalism (Fisher-Lee formula) together with the density functional based tight-binding method (Figure 3 bottom).<sup>[26–28]</sup> The rippling induces a dramatic reduction in the conductance of MoS<sub>2</sub> monolayers again independent of the system size. On average the conductance is reduced by 75% in the most rippled structures with respect to the completely flat ones (Figure 3 solid and dashed green line). A monotonic reduction of the conductance with respect to the system length/size has been observed for both flat and rippled structures as expected given the formalism used to compute the conductance.

These results may contribute to the rather strong performance dependence of MoS<sub>2</sub> monolayers on production technique and importantly on the choice of substrate and top layer materials. The degree of rippling will certainly be influenced by interlayer interactions, and hence the choice of substrate may not only act as dielectric, but also influence the degree of MoS<sub>2</sub> rippling and hence the device performance.

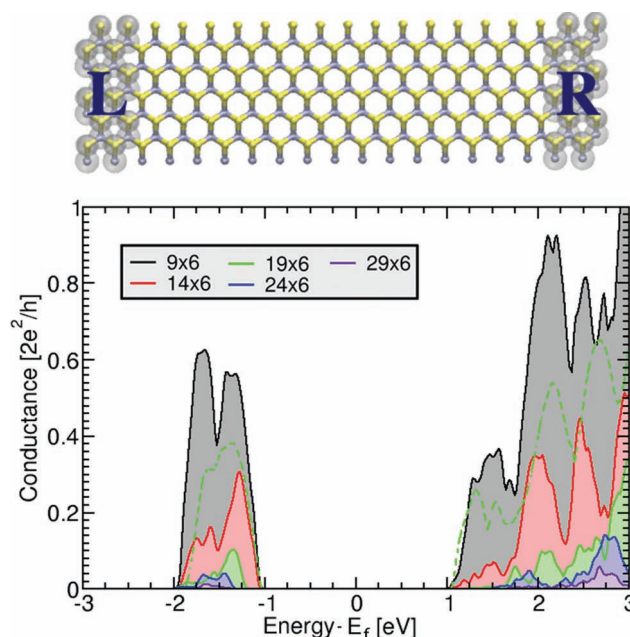


**Figure 3.** Electron conductance (in  $2e^2/h$ ) of the rippled monolayers (bottom). conductance of the flat  $19 \times 6$  monolayer is presented by the green dashed line. Fermi energy level ( $E_F$ ) shifted to 0 eV. Note: The bandgap in the plot belongs to the electrodes that are perfectly flat (see Supporting Information).

In conclusion, we demonstrated the inherent dynamics of MoS<sub>2</sub> monolayers lead to the spontaneous formation of ripples even at low temperatures. The ripples average height is directly influenced by the size of the simulated system, converging to the height observed experimentally for supercells with lengths of ca. 91 Å and we confirmed the origin of thermal ripple formation. Both the bandgap and electron conductance are significantly reduced due to monolayer deformation. Our results are in agreement with those reported for the mechanical deformation of this material.<sup>[25]</sup>

Strain effects have been suggested as a possible way of tuning bandgaps and transport properties of transition metal dichalcogenides monolayers. However our results demonstrate that further studies are required to fully understand and control the inherent dynamics of these materials towards their application in optoelectronics or nanosensor device engineering. In consequence, studies are ongoing in our group to address the rippling of deposited monolayers, multilayered systems and the influence of defects (point or line).

## Supporting Information

Supporting Information is available from the Wiley Online Library or from the author.

## Acknowledgements

This work was supported by the German Research Council (Deutsche Forschungsgemeinschaft, HE 3543/18-1), The European Commission (FP7-PEOPLE-2009-IAPP QUASINANO, GA 251149 and FP7-PEOPLE-2012-ITN MoWSeS, GA 317451).

Received: April 4, 2013

Revised: May 17, 2013

Published online: July 1, 2013

- [1] a) E. M. Lifshitz, L. P. Pitaevskii, *Statistical Physics Part I*; Pergamon: Oxford: U.K 1980; b) L. D. Landau, E. M. Lifshitz, L. P. Pitaevskii, *Statistical Physics Part II*; Pergamon: Oxford: U.K 1980.
- [2] a) R. E. Peierls, *Ann. Inst. Henri Poincaré* **1935**, 5, 177; b) R. E. Peierls, *Helv. Phys. Acta* **1934**, 7, 81.
- [3] N. D. Mermin, H. Wagner, *Phys. Rev. Lett.* **1966**, 17, 1133.
- [4] H. P. Boehm, A. Clauss, G. O. Fischer, U. Hofmann, *Z. Anorg. Allg. Chem.* **1962**, 316, 119.
- [5] K. S. Novoselov, A. K. Geim, S. V. Morozov, D. Jiang, Y. Zhang, S. V. Dubonos, I. V. Grigorieva, A. A. Firsov, *Science* **2004**, 306, 666.
- [6] K. S. Novoselov, A. K. Geim, S. V. Morozov, D. Jiang, M. I. Katsnelson, I. V. Grigorieva, S. V. Dubonos, A. A. Firsov, *Nature* **2005**, 438, 197.
- [7] J. C. Meyer, A. K. Geim, M. I. Katsnelson, K. S. Novoselov, T. J. Booth, S. Roth, *Nature* **2007**, 446, 60.
- [8] A. Fasolino, J. H. Los, M. I. Katsnelson, *Nat. Mater.* **2007**, 6, 858.
- [9] D. Pacile, J. C. Meyer, C. O. Girit, A. Zettl, *App. Phys. Lett.* **2008**, 92.
- [10] J. C. Meyer, A. Chuvilin, G. Algara-Siller, J. Biskupek, U. Kaiser, *Nano Lett.* **2009**, 9, 2683.
- [11] J. N. Coleman, M. Lotya, A. O'Neill, S. D. Bergin, P. J. King, U. Khan, K. Young, A. Gaucher, S. De, R. J. Smith, I. V. Shvets, S. K. Arora, G. Stanton, H. Y. Kim, K. Lee, G. T. Kim, G. S. Duesberg, T. Hallam, J. J. Boland, J. J. Wang, J. F. Donegan, J. C. Grunlan, G. Moriarty, A. Shmeliov, R. J. Nicholls, J. M. Perkins, E. M. Grieveson, K. Theuwissen, D. W. McComb, P. D. Nellist, V. Nicolosi, *Science* **2011**, 331, 568.
- [12] M. Chhowalla, H. S. Shin, G. Eda, L. J. Li, K. P. Loh, H. Zhang, *Nat. Chem.* **2013**, 5, 263.
- [13] Q. H. Wang, K. Kalantar-Zadeh, A. Kis, J. N. Coleman, M. S. Strano, *Nat. Nanotechnol.* **2012**, 7, 699.
- [14] K. S. Novoselov, D. Jiang, F. Schedin, T. J. Booth, V. V. Khotkevich, S. V. Morozov, A. K. Geim, *Proc. Natl. Acad. Sci. USA* **2005**, 102, 10451–10453.
- [15] H. S. S. R. Matte, A. Gomathi, A. K. Manna, D. J. Late, R. Datta, S. K. Pati, C. N. R. Rao, *Angew. Chem. Int. Ed.* **2010**, 49, 4059.
- [16] H. Topsoe, B. S. Clausen, F. E. Massoth, *Hydrotreating Catalysis, Science and Technology*; Springer-Verlag: Berlin **1996**.
- [17] J. V. Lauritsen, M. Nyberg, J. K. Nørskov, B. S. Clausen, H. Topsoe, E. Laegsgaard, F. Besenbacher, *J. Catal.* **2004**, 224, 94.
- [18] S. Gemming, G. Seifert, *Nat. Nanotechnol.* **2007**, 2, 21.
- [19] Q. H. Wang, K. Kalantar-Zadeh, A. Kis, J. N. Coleman, M. S. Strano, *Nat. Nanotechnol.* **2012**, 7, 699.
- [20] K. F. Mak, C. Lee, J. Hone, J. Shan, T. F. Heinz, *Phys. Rev. Lett.* **2010**, 105.
- [21] M. Stefanov, A. N. Enyashin, T. Heine, G. Seifert, *J. Phys. Chem. C* **2008**, 112, 17764.
- [22] B. Radisavljevic, A. Radenovic, J. Brivio, V. Giacometti, A. Kis, *Nat. Nanotechnol.* **2011**, 6, 147–150.
- [23] J. Brivio, D. T. L. Alexander, A. Kis, *Nano Lett.* **2011**, 11, 5148.
- [24] A. Kuc, N. Zibouche, T. Heine, *Phys. Rev. B* **2011**, 83.
- [25] M. Ghorbani-Asl, S. Borini, A. Kuc, T. Heine, *Phys. Rev. B* **2013**, DOI 10.1103/PhysRevB.00.005400.
- [26] D. S. Fisher, P. A. Lee, *Phys. Rev. B* **1981**, 23, 6851.
- [27] M. P. L. Sancho, J. M. L. Sancho, J. Rubio, *J. Phys F* **1985**, 15, 851.
- [28] S. Datta, *Quantum Transport: Atom to Transistor*, 2nd ed., Cambridge University Press: Cambridge and New York **2005**.